Preparation By Grafting Onto, Characterization, and Properties of Thermally Responsive Polymer-Decorated Cellulose Nanocrystals

ARTICLE *in* BIOMACROMOLECULES · NOVEMBER 2010

Impact Factor: 5.75 · DOI: 10.1021/bm101106c · Source: PubMed

4 AUTHORS, INCLUDING:

Jean-Luc Putaux
French National Centre for Scientific Resea…

178 PUBLICATIONS **5,167** CITATIONS

SEE PROFILE

Preparation By Grafting Onto, Characterization, and Properties of Thermally Responsive Polymer-Decorated Cellulose Nanocrystals

Firas Azzam,[†] Laurent Heux,[†] Jean-Luc Putaux,[†] and Bruno Jean*[,†]

Centre de Recherches sur les Macromolécules Végétales (CERMAV-CNRS), BP 53, 38041 Grenoble Cedex 9, France

Received September 17, 2010; Revised Manuscript Received October 15, 2010

The grafting of thermosensitive amine-terminated statistical polymers onto the surface of cellulose nanocrystals (CNCs) was achieved by a peptidic coupling reaction, leading to unusual properties like colloidal stability at high ionic strength, surface activity, and thermoreversible aggregation. We have used a large variety of experimental techniques to investigate the properties of the polymer-decorated CNCs at different length-scales and as a function of the different reaction parameters. A high grafting density could be obtained when the reaction was performed in DMF rather than water. Infrared and solid-state NMR spectroscopy data unambiguously demonstrated the covalent character of the bonding between the CNCs and the macromolecules, whereas TEM images showed a preserved individualized character of the modified objects. Dynamic light scattering and zeta potential measurements were also consistent with individual nanocrystals decorated by a shell of polymer chains. Surface tension measurements revealed that CNCs became surface-active after the grafting of thermosensitive amines. Decorated CNCs were also stable against high electrolyte concentrations. A thermoreversible aggregation was also observed, which paves the way for the design of stimuli-responsive biobased nanocomposite materials.

Introduction

A key scientific and technological issue is the design of new composite materials based on renewable natural resources. These materials will have to replace toxic or nonbiodegradable materials derived from fossil resources, while offering similar mechanical, thermal, or optical properties. In this framework, cellulose nanocrystals (CNCs)[1] are attracting growing attention due to their unique properties: prepared by acid hydrolysis of extremely abundant native cellulose microfibrils, they are crystalline nanorods with a high aspect ratio, a low density, a high specific surface area in the 150−300 m^2/g range,[2,3] and excellent mechanical properties.[4−6] The CNCs are, thus, ideal building blocks to be used in a bottom-up strategy for the design of hierarchical materials with tunable properties. CNCs are usually prepared by sulfuric acid hydrolysis that yields aqueous suspensions of negatively charged nanoparticles.[7−10] Converting the electrostatically stabilized CNC suspensions into sterically stabilized systems would impart new properties to these objects and extend their range of application. Indeed, steric stabilization presents several advantages when compared to electrostatic stabilization: (i) the steric repulsion is insensitive to the electrolyte concentration whereas the charge-stabilized colloids flocculate at high ionic strength; (ii) the steric stabilization is effective both in aqueous and nonaqueous media; (iii) the steric stabilization is effective over a wide range of volume fractions of colloid particles and should prevent the early onset of a glassy phase, often observed in concentrated suspensions of charged colloids.

Steric stabilization of colloids is usually achieved by adsorption or surface grafting of polymer chains. Neutral polymers adsorbed or grafted to a surface expand away to gain configurational entropy. When a chain emanating from a surface encounters a chain from another surface, its allowed conformations are reduced and its tendency to increase its configurational entropy provides resistance to further compression. So-called steric or entropic repulsion between surfaces are thus generated as the grafted polymer layers overlap. Generally, the repulsion force appears once a surface−surface separation distance of the order of twice the radius of gyration of the chains, R_g, is reached. The dimensions of the polymer coil therefore determine the range of the entropic force.

In this study, we have used a "grafting onto" strategy consisting in creating a covalent amide bond between a primary amine-terminated polymer and carboxylated CNCs by peptidic coupling. This method has already been successfully applied to the grafting of PEG or DNA oligonucleotides to the surface of CNCs and of amine derivatives onto cellulose microfibrils.[11−13] It is divided into two main steps: (i) a TEMPO-catalyzed selective oxidation of primary hydroxyl groups on the surface of CNCs yielding carboxyl units; (ii) a coupling with amine derivatives by a peptidic coupling reaction using a carbodiimide as amidation agent. The grafting of polyethylene glycol (PEG) chains by Araki et al. resulted in sterically stabilized CNCs, while Mangalam et al. obtained duplexed CNC structures from the use of cDNA strands.[13] Recently, Kloser and Gray also prepared sterically stabilized PEG-grafted CNCs from the reaction of desulfated CNCs with epoxy-terminated PEG under alkaline conditions.[14] The alternative strategy for the functionalization of the surface of CNCs with macromolecules is the "grafting from" method that has mainly been used to graft hydrophobic polymers like polystyrene[15−17] and recently thermoresponsive chains of poly(*N*,*N*-dimethylaminoethyl methacrylate)[18] or poly(*N*-isopropylacrylamide).[19]

Here, we have focused on the grafting of commercial statistical copolymers of ethylene oxide (EO) and propylene

* To whom correspondence should be addressed. E-mail: bruno.jean@cermav.cnrs.fr.

[†] CERMAV-CNRS (Affiliated with Université Joseph Fourier and member of the Institut de Chimie Moléculaire de Grenoble).

10.1021/bm101106c
Published on Web 11/08/2010

oxide (PO), named Jeffamines (Huntsman Corporation), that possess several interesting properties. First, these polymers exhibit a thermosensitive behavior with a lower critical solution temperature (LCST) that depends on the EO/PO ratio. When a Jeffamine solution is heated above the LCST, the macromolecules undergo a reversible phase separation from a swollen coil to a collapsed globule.[20] Second, Jeffamines originally possess a primary amine terminal moiety, which avoids a lengthy chemical functionalization step. The wide range of molecular weights and the LCST dependence on chemical composition of these macromolecules should provide a wide range of versatile thermal behavior.

In this paper, we describe the grafting of thermosensitive Jeffamine macromolecules on the surface of CNCs using a "grafting onto" strategy and the characterization of the new objects at different length-scales along the various steps of the process. Emphasis has been put on the investigation of the covalent nature of the bonding between the CNCs and the polymer chains. It is indeed of utmost importance to achieve a permanent linkage between both species and to avoid contamination by ungrafted chains. Conductometric titration, infrared, and solid-state NMR spectroscopies were used to probe the functionalization of the nanocrystals. Transmission electron microscopy (TEM), dynamic light scattering (DLS), and zeta potential measurements were used to investigate the structural modifications of the nanoparticles. Surface tension measurements as well as stability and temperature sensitivity tests were performed to investigate the new properties of the systems.

Experimental Section

Materials. Cotton linters were provided by Buckeye Cellulose Corporation and used as the cellulose source without any further purification. Jeffamines M1000, M2070, and M2005 statistical copolymers were donated by Huntsman Corporation. Their PO/EO compositions are 3/19, 10/31, 29/6, their molecular weights 1000, 2070, and 2005 g/mol and their LCST ~80, ~70 and ~16 C, respectively. Other chemicals were purchased from Sigma-Aldrich. Anhydrous DMF was obtained by using thoroughly dried 15A molecular sieves. Deionized water was used for all experiments.

Preparation of Cellulose Nanocrystals by Acid Hydrolysis. To prepare CNC suspensions, cotton linters were hydrolyzed according to the method described by Revol et al. by treating the almost pure cellulosic substrate with 65% sulfuric acid during 30 min at 63 C.[10] The suspensions were washed by repeated centrifugations, dialyzed against distilled water until neutrality, and ultrasonicated for 4 min with a Branson B-12 Sonifier equipped with a 3 mm microtip. After these treatments, the suspensions were filtered through 8 μm and then 1 μm cellulose nitrate membranes (Sartorius). At the end of the process, ~3 wt % stock suspensions were obtained.

Carboxylation of Cellulose Nanocrystals by TEMPO Oxidation. Cellulose nanocrystals resulting from sulfuric acid hydrolysis of cotton linters were subjected to TEMPO-mediated oxidation as previously reported.[21−23] NaBr (1.588 g, 15.4 mmol) and TEMPO (135 mg, 0.86 mmol) were added to 500 mL of a 1 wt % cellulose nanocrystals suspension (30.8 mmol anhydroglucose units) and magnetic stirring was applied for 1 h. A total of 21.1 mL of a 1.46 M NaOCl solution (1 equiv per anhydroglucose unit) was then added dropwise under stirring to the cellulose suspension. During NaOCl addition, the pH was maintained at 10 using a 0.5 M NaOH solution. The reaction was stopped when the pH was constant by adding methanol (20 mL) and the pH was adjusted to 7 with 0.5 M HCl. The obtained suspensions were washed three times with distilled water by centrifugation at 20000 g and redispersion. NaCl (0.5 M) was added to facilitate the nanoparticles separation and the washing procedure was repeated three times using a 0.1 N HCl solution. After dialysis against distilled water, a stable colloidal suspension was obtained.

Preparation of Stable Suspensions of Cellulose Nanocrystals in DMF. To test the role of the solvent on the polymer coupling yield, we first investigated the redispersion of the carboxylated cellulose nanocrystals in DMF. Aqueous dispersions of carboxylated CNCs were then solvent-exchanged, first with acetone and then with DMF by centrifugation-redispersion. Acetone (100 mL) was added to a centrifugation beaker containing an aqueous dispersion of carboxylated CNCs (50 mL, 1 wt %). The mixture was agitated for 30 min and centrifuged at a speed of 11200 rpm at a temperature of 4 C. The supernatant was removed and the CNCs sediment was redispersed in 50 mL of acetone and agitated for 30 min. After three successive mixings with acetone followed by centrifugation, the CNCs sediment was mixed with 50 g of DMF and agitated for about 1 h until obtaining a stable suspension that was ultrasonicated for 4 min.

Polymer Grafting by Peptidic Coupling in Water. Grafting of amine-terminated Jeffamine was achieved through peptidic coupling according to Bulpitt and Aeschlimann.[24] The pure polymer was added (N_p moles per carboxyl unit measured by conductometry) to a 1 wt % carboxylated CNC suspension and stirred until dissolution. The reaction was performed at room temperature for Jeffamine M1000 and M2070 and at 4 C for Jeffamine M2005 to ensure that the macromolecules were under good solvent conditions. The pH was adjusted to 7.5−8.0 before the addition of 2 mL of an aqueous solution containing *N*-(3-dimethylaminopropyl)-*N*′-ethylcarbodiimide hydrochloride (EDAC) and *N*-hydroxysuccimide (NHS; N_{EDAC} and N_{NHS} mol per carboxyl group, respectively). Unless otherwise stated, all results were obtained with $N_P = N_{EDAC} = N_{NHS} = 4$. The reaction lasted 24 h at room temperature under stirring while maintaining the pH of the mixture at 7.5−8.0 using 0.5 M NaOH or 0.5 M HCl. The pH was finally decreased to 1−2 by addition of 0.5 M HCl and the resulting suspension was dialyzed against distilled water to remove excess reagents including nongrafted Jeffamine.

Polymer Grafting by Peptidic Coupling in DMF. Grafting of Jeffamine polymers on the nanocrystal surface in DMF was performed using the same protocol as in water, except that no pH adjustment was done. Furthermore, the washing procedure was reduced to an extensive dialysis against distilled water to remove reagents in excess and to exchange the solvent (from DMF to water). The polymer grafting reaction was then performed in DMF but an aqueous dispersion was recovered at the end of the process.

Carboxyl Content. The carboxyl content of the samples after TEMPO oxidation was determined using conductometric titration. The CNC suspensions were first treated with an excess of HCl to replace the sodium counterions by protons. The acidified suspensions were then titrated with 0.01 M NaOH using a CDM 210 conductimeter equipped with a CDM 614T electrode. The titration curves exhibit two discontinuities, the first one corresponding to the presence of strong acid due to the excess of HCl and a second one attributed to weak acid and related to the carboxyl content. These data allowed us to calculate the degree of oxidation (DO) according to the equation given by da Silva Perez et al.[25] DO is the number of primary hydroxyl groups that have been oxidized into carboxyl groups per anhydroglucose unit. During the peptidic coupling with polymer chains, some of the carboxyl groups are consumed in the reaction with the polymer chain end. Therefore, a measure of the carboxyl content after polymer grafting gave a new degree of oxidation, DO1, such as DO1 ≤ DO. The degree of substitution, DS, was defined as DO − DO1 and represents the number of carboxylic groups that have been replaced by a polymer chain per anhydroglucose unit. Another useful quantity is given by 100 × DS/DO, which represents the percentage of carboxyl groups that have reacted with a polymer chain end, that is, the peptidic coupling yield.

Transmission Electron Microscopy. Drops of about 0.001 wt % CNC suspensions were deposited onto glow-discharged carbon-coated TEM grids. After 2 min, the liquid in excess was absorbed with filter paper and, prior to drying, a drop of 2% uranyl acetate was deposited on the specimen. After 2 min, the stain in excess was blotted and the remaining thin liquid film was allowed to dry. The specimens were

observed using a Philips CM200 electron microscope operating at 80 kV. The images were recorded on Kodak SO163 films.

Solid-State NMR. NMR experiments were performed with a Bruker Avance DSX 400 MHz spectrometer operating at 100.6 MHz for ^{13}C, using the combination of cross-polarization, high-power proton decoupling and magic angle spinning (CP/MAS) methods. The spinning speed was set at 12000 Hz. The ^{1}H radio frequency field strength was set to give a 90 pulse duration at 2.5 μs. The ^{13}C radio frequency field strength was obtained by matching the Hartman−Hahn conditions at 60 kHz. Recording at least 2000 transients with contact time and recycle delay, respectively, of 2 ms and 2 s represented standard conditions. The acquisition time was set at 30 ms and the sweep width at 29400 Hz. The deconvolution of the spectra was achieved following an earlier procedure.[26] The position and width of the lines were maintained constant throughout a series of samples. The area corresponding to the integration of the C1 signal was used as an internal standard and set to one.

Surface Tension. Surface tension measurements were performed using the rising bubble method with a Tracker instrument from IT Concept (France). A rising air bubble was produced at the end of a tip in the thermostatted solution under investigation and the profile of the air drop was monitored with a camera and then analyzed by a dedicated software. The Laplace equation was used to calculate the value of the surface tension from the radius of the drop.

Fourier-Transform Infrared Spectroscopy. CNC suspensions were first acidified to pH 2−3 to avoid the superposition of the carbonyl band with that of water and then freeze-dried. KBr pellets containing 1 wt % solid cellulose sample were prepared and spectra were recorded in transmission mode using a Perkin-Elmer 1720X FTIR apparatus in the 400−4000 cm^{-1} wavenumber range.

Dynamic Light Scattering. DLS experiments were carried out with a Malvern NanoZS instrument. Unless otherwise stated, all measurements were made at a temperature of 25 C with a detection angle of 173 . The intensity size distribution was obtained from the analysis of the correlation function using the multiple narrow mode algorithm of the Malvern DTS software.

Zeta Potential. The zeta potential was measured by electrophoresis coupled with laser Doppler velocimetry using a Malvern NanoZS instrument. All samples were measured at pH 7 and 0.01 M NaCl. Data were averaged over three measurements.

Results and Discussion

TEMPO Oxidation of Cellulose Nanocrystals. Aqueous CNC suspensions obtained from sulfuric acid hydrolysis of cotton linters were carboxylated using the now well-established TEMPO oxidation method. A degree of oxidation DO of 0.196 (mol/mol of anhydroglucose unit) was obtained, which is comparable to the one previously measured with the same oxidation conditions.[12] Moreover, the value of ~0.2 is close to the maximum DO, related to the surface-to-volume ratio of the crystals, which can be reached in the case of cotton cellulose nanocrystals.[27]

Cellulose Nanocrystal Suspensions in DMF. Using the method described in the Experimental Section, we prepared CNC suspensions in DMF at a concentration of 0.5−1.5 wt % that were characterized at different length scales. First, at a macroscopic scale, naked-eye observation of the suspensions over several weeks showed no sedimentation, demonstrating that suspensions as stable as aqueous ones were obtained. Second, the test of flow birefringence observed between crossed polars was performed.[28] As shown in Supporting Information, Figure S1, the flow birefringence of CNC suspensions in DMF did not reveal any large aggregate. Third, nanometric scale characterizations were performed using DLS and TEM. 0.1 wt % dilute CNC suspensions in water and in DMF were investigated by DLS. The corresponding nanoparticle size distributions are plotted in Figure 1. In both cases, a monomodal size distribution centered around 130 nm was found, showing the absence of aggregates. These results proved that the dispersion quality was as good in DMF as in water. Because DLS measures the diffusion coefficient of the particles, which is then converted into a hydrodynamic radius from the Stokes−Einstein equation, the size given by this technique is therefore the radius of a sphere having the same diffusion coefficient as the rodlike CNCs. The size of about 130 nm given by DLS is close to the average length determined by Elazzouzi-Hafraoui et al. for cotton CNCs.[29] TEM micrographs of cotton CNCs from aqueous and DMF dispersions are shown in Figure 2a and b, respectively. No aggregates are observed and the crystallites are well individualized in both cases. Therefore, from these characterizations, it can be concluded that the centrifugation/redispersion method resulted in very good dispersions of CNCs in DMF. It has to be noted that DMF is an aprotic solvent with a rather high dielectric constant ($\varepsilon = 38$), which makes charge separation still possible. The method used here might not be transposed to apolar solvents with low dielectric constants such as toluene.

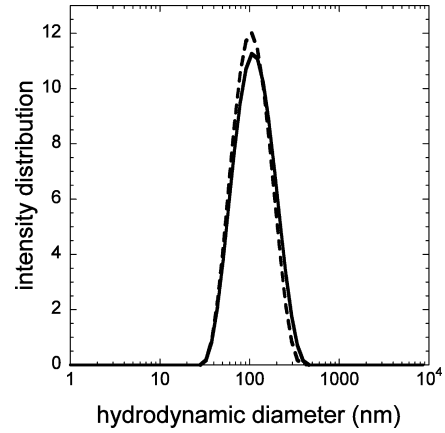

Figure 1. Intensity distribution of a 0.1 wt % suspension of cellulose nanocrystals from cotton in water (solid line) and in DMF (dashed line) measured by DLS.

The ability of CNCs derived from sulfuric acid hydrolysis to be dispersed in organic solvents has been investigated by several groups. Van den Berg et al. prepared stable suspensions of tunicin whiskers in polar aprotic solvents such as DMF using freeze-drying followed by a sonication-assisted redispersion but this method requires high energy input that can damage the nanocrystals.[30] This case cannot directly be compared with our method because tunicin nanocrystals largely differ from cotton nanocrystals in terms of size, aspect ratio, and charge density. Viet et al. showed that, in the case of freeze-dried cotton CNCs, a minimum amount of water should be present in the redispersion solvent (DMSO or DMF) to achieve a good dispersion.[28] However, in our case, oxidized nanocrystals could be redispersed as easily in commercial DMF with a very small amount of water (<0.1%) or in anhydrous DMF (data not shown). Weder and co-workers also developed an efficient but time-consuming solvent exchange sol−gel process that makes the dispersion of cotton or tunicin nanocrystals in DMF possible.[31]

Grafting of Jeffamines onto CNCs. The degree of substitution (DS) and peptidic coupling reaction yield (DS/DO) after reaction of the carboxylated CNCs with the Jeffamines are reported in Table 1 as a function of the type of solvent and Jeffamine used.

Effect of Solvent. DS/DO values are significantly larger in DMF (26−53%) than in water (20−30%). It can clearly be concluded that the coupling reaction is favored in DMF,

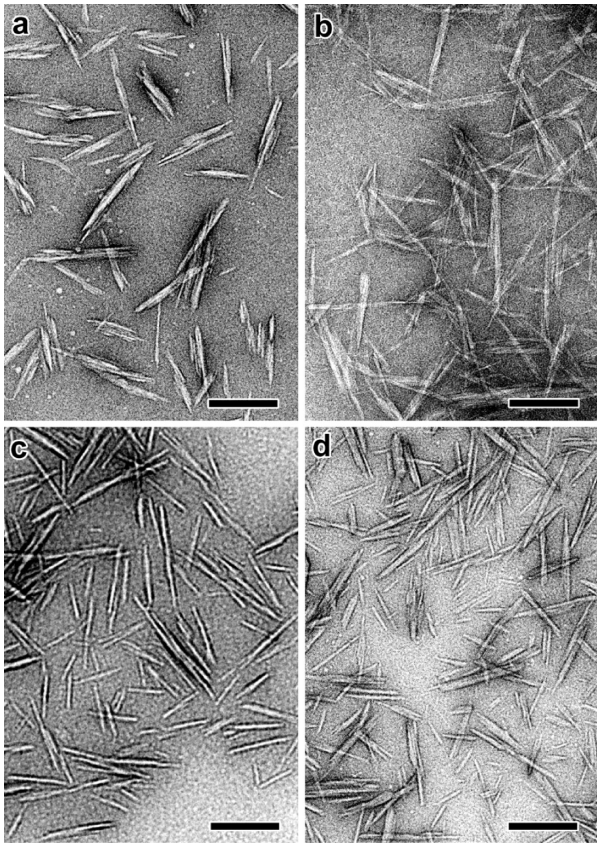

Figure 2. TEM micrographs of negatively stained cellulose nanocrystals: oxidized suspended in water (a), oxidized suspended in DMF (b), M1000-grafted suspended in water (c), and M2070-grafted suspended in water (d). Grafting reactions were performed in DMF for M1000 and in water for M2070. The scale bar is 200 nm.

allowing to reach higher degrees of coupling. As observed for peptide synthesis, DMF prevents competition between the solvent and the polymer for the reaction with the CNC surface.[32]

Effect of the Type of Jeffamine. The grafting of three different amine-terminated polymers, Jeffamines M1000, M2070, and M2005, has been investigated. Composition and molecular weights of these polymers are reported in the Experimental Section. The data presented in Table 1 show that Jeffamine M1000 is systematically more reactive than Jeffamine M2070, yielding higher DS and DS/DO values. For equivalent reaction times, this effect can be attributed to the higher mobility of Jeffamine M1000 in the reaction medium, because it has a lower molecular weight. Even if both polymers are soluble in water and DMF, they have a different hydrophobicity. Jeffamine M1000 has a lower PO/EO ratio and is therefore more hydrophilic than Jeffamine M2070. This difference does not seem to play a major role because M1000 is more reactive than M2070, both in water and DMF.

Effect of the Molar Ratio of Reagents. The coupling reaction involves EDAC as a catalyst and NHS as an agent to prevent formation of stable *N*-acylurea that would reduce the reaction yield. It can be seen in Table S1 (Supporting Information) that for a given solvent, the molar ratios N_P, N_{EDAC}, and N_{NHS} of polymer, NHS, EDAC to carboxyl group, respectively, have an influence on the degree of substitution. Even if the study is not exhaustive, the clear trend is an increase in grafting density with the molar ratios N_P, N_{EDAC}, and N_{NHS}. A similar effect has been observed by Mangalam et al.[13] for the grafting of DNA oligomers onto CNCs where an optimum grafting yield was obtained at a 5 molar excess of EDAC ($N_{EDAC} = 5$) and at a 4 molar ratio DNA/COOH ($N_P = 4$). All results discussed here were obtained with $N_P = N_{EDAC} = N_{NHS} = 4$ because these values lead to the highest degrees of polymer coupling.

The measurement of the degree of coupling by conductimetry is based on the decrease of the number of carboxyl groups after reaction with the amine-terminated polymer. Therefore, it is only an indirect proof of the grafting. FTIR spectroscopy and solid-state NMR were thus used to check the covalent nature of the link between the polymer chains and the nanocrystals. Figure 3 shows FTIR spectra measured using KBr pellets of the hydrolyzed (Figure 3a) and oxidized (Figure 3b) CNCs as well as those grafted with Jeffamines M2070 (Figure 3c), M1000 (Figure 3d), and M2005 (Figure 3e). In this case, the coupling reactions were performed in water. Clear changes occur upon the different chemical treatments. When compared to the hydrolyzed sample, the oxidized one displayed an extra strong absorption band at 1736 cm^{-1} that is characteristic of the carboxyl groups in their acidic form, thus validating the oxidation. In the spectra corresponding to the grafted samples (Figure 3c−e), the intensity of this band is significantly reduced, revealing the consumption of carboxyl groups in the reaction with the amine-terminated polymers. The grafted samples also display a band around 1650 cm^{-1} that can both be attributed to the amide bond (amide I absorption band) or to residual water. However, when compared to the oxidized sample, the pronounced increase of this band should at least partly be due to the amide bond. Moreover, the new absorption band at 1550 cm^{-1} for the grafted samples unambiguously corresponds to the N−H stretching in the amide bond (called amide II). For the three polymers, these features prove the effective covalent grafting of the macromolecules on the CNC surface through amide bonding. The high intensity of the 1550 cm^{-1} band is particularly striking. These results were confirmed using FTIR spectroscopy in reflectance mode (see Supporting Information).

Further evidence of the effective grafting was provided by solid-state NMR spectroscopy. Figure 4 shows spectra prior (oxidized) and after grafting with Jeffamines. Cellulose I signals for both oxidized and grafted nanocrystals are identical to those reported in the literature.[27,33−35] The region from 60 to 70 ppm is assigned to the hydroxymethyl C6 carbons, split in a 62 ppm contribution from the disordered chains mainly at the surface and 65 ppm signal arising from the crystalline core.[26,36] The region between 70 and 80 ppm is assigned to C2, C3, and C5 carbons that are undistinguishable. The following region from 80 to 91 is attributed to C4 carbons, where the wide signal at 83 ppm is assigned to the C4 carbons of disordered cellulose chains and the sharp signals at 88 ppm to crystalline ones. Finally, the region around 105 ppm corresponds to C1 carbons of native cellulose. As reported by Montanari et al.,[27] the oxidized sample is characterized by the signal of the carboxylic acid at around174 ppm.

Upon grafting, important changes occur and several new signals appear. First, a new signal arises at 170 ppm at the expense of the carboxylic acid peak at 174 ppm. This signal most probably corresponds to the C6 carbon in its amide form, indicating the formation of the amide covalent linkage from the reaction of the carboxylic acid with the terminal primary amine of a Jeffamine macromolecule.[12] Another new signal is observed at 155 ppm. The most likely explanation for this peak is the formation of an imine linkage between the amine group of a Jeffamine chain and an aldehyde group on the nanocrystal surface.[37−39] In fact, Saito et al. reported that TEMPO oxidation, which is selective for the primary alcohol functions of the native cellulose, does not only generate carboxylic acid but also

Table 1. Reaction Parameters and Characterization for the Grafting of Polymer Chains onto Cellulose Nanocrystals

sample	reaction solvent	grafted polymer	DS[a]	100 × DS/DO[b] (%)	D_h[c] (nm)	ζ[d] (mV)	γ_{eq}[e] (mN/m)
Ssulf	water	nongrafted/sulfated			133.5	−26.9	
Sox	water	nongrafted/oxidized			133.9	−23.5	
S1000W	water	M1000	0.059	30.1	141.1	−8.41	46 ± 1.5
S2070W	water	M2070	0.0419	21.4	145.5	−5.76	36 ± 1.5
S1000D	DMF	M1000	0.1049	53.5	190.0	−4.49	41 ± 1.5
S2070D	DMF	M2070	0.0973	49.6	154.0	−12.7	39 ± 1.5

[a] Degree of substitution (DS). [b] Peptidic coupling yield (DS/DO) measured by conductometry. [c] Hydrodynamic diameter measured by dynamic light scattering. [d] Zeta potential. [e] Equilibrium surface tension. The initial degree of oxidation (DO) was 0.196.

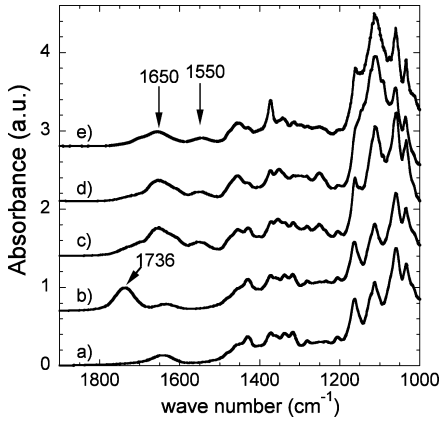

Figure 3. Infrared spectra of sulfated (a), oxidized (b), M1000-grafted (c), M2070-grafted (d), and M2005-grafted (e) cellulose nanocrystals.

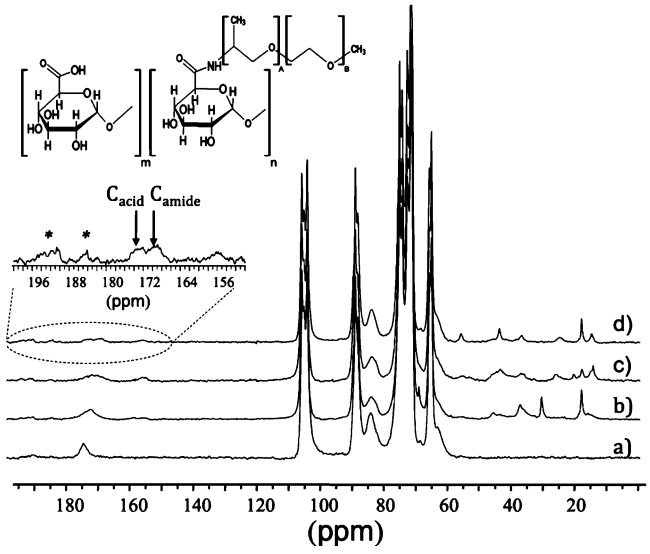

Figure 4. ^{13}C solid-state NMR spectra of oxidized (a), M2070-grafted in water (b), M1000-grafted in DMF (c), and M2005-grafted in DMF (d) cellulose nanocrystals. Asterisks designate residual side bands.

aldehyde groups, accounting for approximately 20% of the total carbonyl groups.[22] It has to be noted that the imine signal at 155 ppm is more pronounced when the grafting reaction is performed in DMF than in water, even if aqueous suspensions are eventually prepared. Imine formation results in the liberation of a water molecule and is consequently not favored in the presence of water. However, excellent yields of imine formation were reported by Simion et al. who investigated the reaction between benzaldehyde and aniline (primary amine) in aqueous solution.[40]

Signals arising from the grafted polymer carbons also appear upon coupling. The signal at 43 ppm corresponds to the first carbon next to the amide linkage (Cα). The signal at 55 ppm is attributed to the terminal methyl carbon. The carbon signals of propylene oxide methyl side group appear at 17 and 19 ppm.

Table 2. Quantitative Analysis of Solid State ^{13}C NMR Spectra

sample	carboxylic acid signal (174 ppm)	amide signal (170 ppm)	imine signal (155 ppm)	100 × DS/DO (%)	CI[a]
Sox	0.103				0.68
S2070W	0.069	0.062		47.3	0.72
S1000D	0.043	0.064	0.022	59.8	0.74
S2005D	0.036	0.057	0.0185	61.3	0.76

[a] Crystallinity index. See text for details.

Signals at 25 and 36 ppm result from the presence of impurities and could be assigned to the EDAC coupling agent used in large excess during the coupling reaction. They approximately account for 2−6% of the total product.

To quantitatively exploit the data, spectra were normalized using the C1 signals (100−105 ppm) as an internal standard, and integration of the signals of interest was achieved after deconvolution of the NMR peaks.[26] Acid and amide signals integration gives the DO (or DO1) and DS values, respectively. The data are summarized in Table 2. For all three samples investigated by solid-state NMR, a high value of DS/DO is observed, with larger values for reactions performed in DMF compared to water, in agreement with conductometric titration measurements. For the S2005D and S1000D samples, the imine signal is not negligible, accounting for 20% of the total oxidized groups, in good agreement with the estimation of aldehyde content of Saito et al.[22] This makes the total number of grafted chains higher than expected from the DS value. The results in Table 2 show that the validity of the equation DO = DO1 + DS is preserved. However, DO values extracted from NMR data are lower than DO values extracted from conductometric titration. The most probable explanation under ongoing investigation is that remaining sulfate ester groups contribute to the DO measured by conductometric titration.

The crystallinity index of the nanoparticles can be estimated by the ratio between the C4 crystalline and the C4 amorphous signals.[26,36] As shown in Table 2, a slight increase in crystallinity is observed upon polymer grafting, most probably due to the solubilization of the most labile amorphous chains. Hirota et al. recently reported on such peeling of surface chains in alkali.[41] This result indicates that the integrity of the nanocrystals is not altered by the polymer coupling reaction.

Colloidal-Scale Characterization of Jeffamine-Grafted CNCs. TEM micrographs of negatively stained polymer-decorated CNCs are shown in Figure 2c and d. By comparison with the bare nanocrystals shown in Figure 2a, it can be concluded that the morphology of the particles has remained unchanged after grafting. It can be noted that polymer-grafted cellulose nanocrystals are very well-dispersed since very few bundles of laterally associated nanocrystals are observed. This high degree of individualization of the nanoparticles can be attributed to the presence of surface polymer chains generating entropic repulsion forces between the nanocrystals. However, the grafted chains could not be visualized around the CNCs,

most probably because their size is too small and their surface density is too low to generate a detectable contrast in the TEM images of dried preparations.

Suspensions of hydrolyzed, oxidized, and grafted CNCs were then investigated by DLS to observe any change in the hydrodynamic size of the particles. Moreover, variations in the zeta potential of the particles were measured to probe the electrical charge environment of the nanocrystals as a function of the different chemical treatments and subsequent surface modifications. Results are summarized in Table 1. The hydrodynamic diameter of hydrolyzed cotton CNCs is about 130 nm. The zeta potential determined for these particles, around −27 mV, is consistent with a stable suspension of negatively charged objects. The charges result from the presence of sulfate groups after sulfuric acid hydrolysis.

The comparison of data for hydrolyzed and oxidized nanocrystals shows that no change in the size of the colloids occurred during the carboxylation step, whereas a moderate increase in zeta potential, from −27 to −23 mV, was observed. The result about the size is expected since no significant variation of the dimensions of the crystals was expected to occur upon oxidation.[27,42] Zeta potential results show that, despite the addition of carboxyl groups upon TEMPO oxidation, the net surface charge of the CNCs decreases. This effect can be attributed to the hydrolysis of sulfate ester groups during the oxidation in alkaline conditions and to the different ionizability of the sulfate and carboxylate groups. The value of about −23 mV after carboxylation is still considered to be large enough to provide electrostatic stability to the suspension and no flocculation of the carboxylated samples was actually observed with such values of the DO. Okita et al. recently reported on the zeta potential values of suspensions of TEMPO oxidized cellulose microfibrils from various origins.[43] Large zeta potential values of about −75 mV were measured. These values were obtained using different conditions than ours and mostly concern microfibrils and not nanocrystals, making comparisons ambiguous.

Grafting Jeffamines onto CNCs influences both their size and zeta potential, whatever the reaction conditions, as shown in Table 1. First, a significant increase in size is revealed by DLS for all the systems. As aforementioned, DLS provides a hydrodynamic diameter resulting from the evaluation of the diffusion coefficient of the particles calculated from the analysis of the self-correlation function. This value has thus no direct geometrical significance in the case of rod-like objects. However, the significant size increase more likely corresponds to a lower diffusion coefficient of the particles, in agreement with a change from bare to polymer-decorated nanocrystals.

For a given Jeffamine, the hydrodynamic radius measured by DLS is higher for samples grafted in DMF than in water, which is in agreement with conductometric and NMR data showing larger grafting densities for reactions performed in DMF. The size increase of the nanocrystals after grafting is expected to depend on the polymer chain length and the grafting density. Even if Jeffamine M2070 has a higher molecular weight than Jeffamine M1000, its grafting density is lower. These two effects probably compensate each other and sizes measured for M2070-grafted samples are not larger than sizes for M1000-grafted samples.

Because moderate grafting densities are obtained, the surface grafted polymer chains should be characterized by a mushroom regime, in which they do not interact. Their size should be of the order of the gyration radius of the macromolecule that can be estimated to 1.5 nm for Jeffamine M2070 and to 1 nm for Jeffamine M1000. As shown by Elazzouzi-Hafraoui et al., the

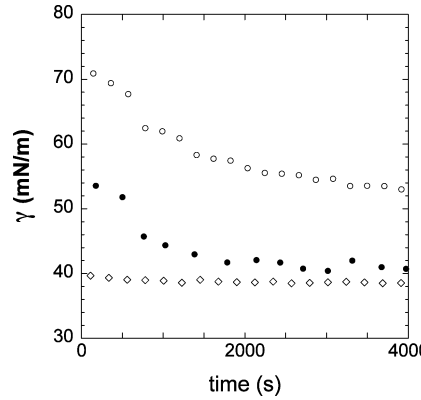

Figure 5. Surface tension as a function of time for a suspension of oxidized nanocrystals (○), a suspension of M1000-grafted CNCs (●) and a solution of Jeffamine M1000 (◇). The concentration is 1 wt % for all samples.

sulfuric acid hydrolysis of cotton linters at 63 C leads to CNCs with average dimensions equal to 128 × 26 × 6 nm^3.[29] Upon grafting, the particle cross-section is therefore expected to increase from 6 to 9 nm in thickness and from 26 to 29 nm in width. For a DS of 0.06, the grafting density can be estimated to 1.2 chain/nm^2, that is, the spacing between neighboring chains is about 1 nm, which is close to the radius of gyration of Jeffamines.

The data in Table 1 reveal for all samples a significant decrease of the absolute value of the zeta potential upon grafting (e.g., from −23 mV for the oxidized sample to −5.76 mV for one M2070-decorated sample). This result demonstrates a severe decrease of the surface charge of the cellulose nanocrystals that is consistent with the consumption of carboxylate units to form the amide bonds with the Jeffamine. The zeta potential results are therefore an indirect proof of the covalent nature of the grafting.

It is generally empirically assumed that electrostatically stabilized suspensions are stable when the absolute value of the zeta potential of the particles is larger than 20 mV. As shown in Table 1, polymer-grafted cellulose nanocrystals exhibit a low zeta potential. Yet, the suspensions of polymer-decorated nanocrystals are stable over weeks. This observation shows that polymer-grafted CNCs are no longer electrostatically but sterically stabilized.

New Properties of Jeffamine-Grafted CNCs. New properties were expected to arise from the grafting of Jeffamines on the surface of CNCs. A possible change in the hydrophilicity of the nanoparticles was investigated by measuring the surface tension of the suspensions at the different steps of the process. Figure 5 shows the evolution of the surface tension with time, $\gamma(t)$, also termed dynamic surface tension, measured from 1 wt % oxidized and M1000-grafted CNC suspensions compared to a 1 wt % solution of Jeffamine M1000. The equilibrium (asymptotic) values of the surface tension, γ_e, for the different samples are listed in Table 1. These data give information on the adsorption kinetics of the dispersed or solubilized species and on the surface-active character of the particles. In the case of Jeffamine M1000 alone, a rapid decrease of γ was observed, within less than 50 s, showing fast adsorption of the rather short polymer chains at the air−water interface. γ_e for Jeffamine M1000 is about 38 mN/m, which corresponds to a highly surface-active species due to the presence of propylene oxide groups along the polymer backbone. For the carboxylated nanocrystals, a much slower decrease of γ with time was measured that is due to a slow diffusion of the large particles

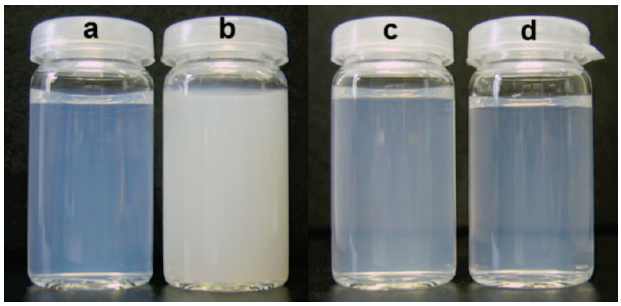

Figure 6. Suspensions of cellulose nanocrystals: (a) oxidized, without salt; (b) oxidized, with 1 M NaCl; (c) M2070-grafted, without salt; (d) M2070-grafted, with 1 M NaCl.

to the interface and their slow rearrangement at the interface. The equilibrium surface tension for oxidized nanocrystals is about 53 mN/M, that is, 19 mN/m lower than the surface tension of pure water, showing the surface-active character of the weakly charged particles. The behavior of Jeffamine M1000-grafted nanocrystals was intermediate between that of the polymer alone and that of the oxidized nanocrystals. The equilibrium surface tension of 41 mN/m is very close to the value for the Jeffamine alone, but equilibrium is reached within 2000 s. Therefore, the affinity for the air−water interface of the decorated nanocrystals is governed by the presence of grafted chains. In comparison with the polymer alone, only the adsorption kinetics seems to be affected, which is easily explained by the slower diffusion coefficient of the nanocrystals bearing the Jeffamines. This experimental observation is again in favor of a covalent association between the Jeffamine and the nanocrystals. Together, these features clearly show that the grafting of Jeffamine has made the particles significantly surface-active. This pronounced modification of the surface activity character of the nanocrystals could be useful for applications in emulsion or foam stabilization.

A second property imparted by the presence of polymer chains on the surface of the nanocrystals is the stability in the presence of an electrolyte. As shown in Figure 6, nongrafted nanocrystals immediately precipitate upon the addition of 1 M NaCl and form a turbid suspension. Conversely, Jeffamine-grafted nanocrystal suspensions remain stable for months in the same conditions. As already shown with PEG-grafted cellulose nanocrystals,[11,14] steric stabilization generated by polymer grafting has remarkable effects on colloidal stability upon electrolyte addition.

Thermosensitive Behavior of CNCs Decorated with Jeffamine M2005. Among the three Jeffamines studied here, M2005 has the highest PO/EO ratio (29/6), which gives this polymer a low LCST. UV/vis absorbance measurements revealed that the LCST of Jeffamine M2005 was between 15 and 20 C, depending on the concentration of the polymer solution (Supporting Information, Figure S3). Since temperature variations within this range can easily be reached experimentally, M2005-grafted samples have been chosen to investigate the effect of temperature on the properties of the suspensions. The hydrodynamic diameter of a M2005-grafted CNC suspension was therefore recorded as a function of temperature and results are shown in Figure 7. When the temperature increased from 4 to 16 C, the hydrodynamic diameter was low and constant. Between 16 and 30 C, a dramatic increase in size was observed, showing the formation of growing aggregates. When the sample was cooled back to 4 C, the hydrodynamic diameter decreased and, at $T \leq 12$ C, recovered a low and constant value similar to the one measured during the heating process. The phenomenon was thus fully reversible even if a 4 C hysteresis was observed. Therefore, the grafting of M2005 polymer chains on the surface of CNCs gave a thermosensitive character to the suspension, as evidenced by the thermoreversible aggregation. When the temperature is below the LCST of Jeffamine M2005, grafted chains are under good solvent conditions, which maximizes steric repulsion forces between particles and results in a dispersion of individual objects. For temperatures higher than the LCST, water becomes a poor solvent for the polymer, first resulting in the individual collapse of the macromolecules.[44] Hydrophobic interactions between collapsed chains can then develop, inducing aggregation of polymer-grafted CNCs. The process is reversible, but the kinetics of association−dissociation involved generates a hysteresis effect.

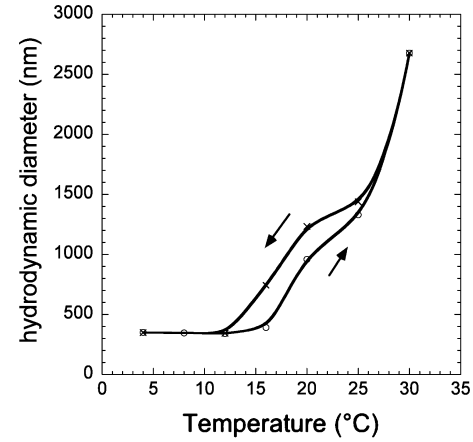

Figure 7. Hydrodynamic diameter as a function of temperature for M2005-grafted cellulose nanocrystals. Heating and cooling are indicated by arrows.

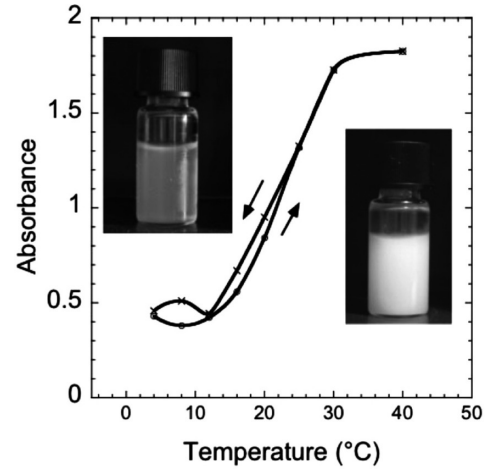

Figure 8. Absorbance at 935 nm vs temperature of a M2005-grafted cellulose nanocrystal suspension. Heating and cooling are indicated by arrows. Images of the suspension at 4 C (left) and at 37 C (right).

The absorbance versus temperature plot determined by UV/vis spectroscopy from a suspension of M2005-grafted CNCs (Figure 8) shows a clear increase of the optical density with temperature above the LCST of the polymer that is in very good agreement with the particle size increase revealed by DLS measurements (Figure 7). As shown by the images, the clear suspension observed at low temperature ($T = 4$ C) turns into a turbid milky suspension at higher temperature ($T = 37$ C). Again, changes in turbidity are reversible with a 4 C hysteresis effect, as observed by DLS.

Conclusion

In this study, thermosensitive Jeffamine copolymers were successfully grafted onto cellulose nanocrystals. Results unambiguously demonstrate the formation of stable covalent amide bonding between the polymer and the particles. The grafting density was sufficiently high to induce a steric stabilization of the CNCs that prevented flocculation at high ionic strength and made the CNCs surface-active. A very interesting feature displayed by the surface-modified CNCs was their thermoreversible aggregation. This property opens the route to the preparation of thermoresponsive biobased materials that would benefit both from the characteristics of the CNCs, such as excellent mechanical properties, and from the stimulus-sensitive character of the grafted chains.

Acknowledgment. B.J. thanks Huntsman Corporation for the generous gift of the Jeffamine samples.

Supporting Information Available. Image of a suspension of CNCs in DMF under crossed polars. Effect of polymer, EDAC, and NHS to carboxyl group molar ratios on the degree of substitution, DS, and peptidic coupling yield, 100 × DS/DO. ATR-IR results for oxidized and M2070-grafted CNCs. Evaluation of the LCST of Jeffamine M2005 using UV absorbance. This material is available free of charge via the Internet at http://pubs.acs.org.

References and Notes

(1) Habibi, Y.; Lucia, L. A.; Rojas, O. J. *Chem. Rev.* **2010**, *110*, 3479–3500.
(2) Ruiz, M. M.; Cavaille, J. Y.; Dufresne, A.; Gerard, J. F.; Graillat, C. *Compos. Interfaces* **2000**, *7*, 117–131.
(3) Angles, M. N.; Dufresne, A. *Macromolecules* **2001**, *34*, 2921–2931.
(4) Eichhorn, S. J.; Young, R. J.; Davies, G. R. *Biomacromolecules* **2005**, *6*, 507–513.
(5) Sturcova, A.; Davies, G. R.; Eichhorn, S. J. *Biomacromolecules* **2005**, *6*, 1055–1061.
(6) Eichhorn, S. J.; Dufresne, A.; Aranguren, M.; Marcovich, N. E.; Capadona, J. R.; Rowan, S. J.; Weder, C.; Thielemans, W.; Roman, M.; Renneckar, S.; Gindl, W.; Veigel, S.; Keckes, J.; Yano, H.; Abe, K.; Nogi, M.; Nakagaito, A. N.; Mangalam, A.; Simonsen, J.; Benight, A. S.; Bismarck, A.; Berglund, L. A.; Peijs, T. *J. Mater. Sci.* **2010**, *45*, 1–33.
(7) Dong, X. M.; Kimura, T.; Revol, J. F.; Gray, D. G. *Langmuir* **1996**, *12*, 2076–2082.
(8) Orts, W. J.; Godbout, L.; Marchessault, R. H.; Revol, J. F. *Macromolecules* **1998**, *31*, 5717–5725.
(9) Revol, J. F.; Bradford, H.; Giasson, J.; Marchessault, R. H.; Gray, D. G. *Int. J. Biol. Macromol.* **1992**, *14*, 170–172.
(10) Revol, J. F.; Godbout, L.; Dong, X. M.; Gray, D. G.; Chanzy, H.; Maret, G. *Liq. Cryst.* **1994**, *16*, 127–134.
(11) Araki, J.; Wada, M.; Kuga, S. *Langmuir* **2001**, *17*, 21–27.
(12) Lasseuguette, E. *Cellulose* **2008**, *15*, 571–580.
(13) Mangalam, A. P.; Simonsen, J.; Benight, A. S. *Biomacromolecules* **2009**, *10*, 497–504.
(14) Kloser, E.; Gray, D. G. *Langmuir* **2010**, *26*, 13450–13456.
(15) Morandi, G.; Heath, L.; Thielemans, W. *Langmuir* **2009**, *25*, 8280–8286.
(16) Xu, Q. X.; Yi, J.; Zhang, X. F.; Zhang, H. L. *Eur. Polym. J.* **2008**, *44*, 2830–2837.
(17) Yi, J.; Xu, Q. X.; Zhang, X. F.; Zhang, H. L. *Polymer* **2008**, *49*, 4406–4412.
(18) Yi, J.; Xu, Q. X.; Zhang, X. F.; Zhang, H. L. *Cellulose* **2009**, *16*, 989–997.
(19) Zoppe, J. O.; Habibi, Y.; Rojas, O. J.; Venditti, R. A.; Johansson, L.-S.; Efimenko, K.; Österberg, M.; Laine, J. *Biomacromolecules* **2010**, *11*, 2683–2691.
(20) Agut, W.; Brulet, A.; Taton, D.; Lecommandoux, S. *Langmuir* **2007**, *23*, 11526–11533.
(21) Denooy, A. E. J.; Besemer, A. C.; Vanbekkum, H. *Recl. Trav. Chim. Pays-Bas* **1994**, *113*, 165–166.
(22) Saito, T.; Isogai, A. *Biomacromolecules* **2004**, *5*, 1983–1989.
(23) Habibi, Y.; Chanzy, H.; Vignon, M. R. *Cellulose* **2006**, *13*, 679–687.
(24) Bulpitt, P.; Aeschlimann, D. *J. Biomed. Mater. Res.* **1999**, *47*, 152–169.
(25) Perez, D. D.; Montanari, S.; Vignon, M. R. *Biomacromolecules* **2003**, *4*, 1417–1425.
(26) Heux, L.; Dinand, E.; Vignon, M. R. *Carbohydr. Polym.* **1999**, *40*, 115–124.
(27) Montanari, S.; Rountani, M.; Heux, L.; Vignon, M. R. *Macromolecules* **2005**, *38*, 1665–1671.
(28) Viet, D.; Beck-Candanedo, S.; Gray, D. G. *Cellulose* **2007**, *14*, 109–113.
(29) Elazzouzi-Hafraoui, S.; Nishiyama, Y.; Putaux, J. L.; Heux, L.; Dubreuil, F.; Rochas, C. *Biomacromolecules* **2008**, *9*, 57–65.
(30) van den Berg, O.; Capadona, J. R.; Weder, C. *Biomacromolecules* **2007**, *8*, 1353–1357.
(31) Tang, L.; Weder, C. *ACS Appl. Mater. Interfaces* **2010**, *2*, 1073–1080.
(32) Cerovsky, V.; Jakubke, H. D. *Biocatalysis* **1994**, *11*, 233–240.
(33) Atalla, R. H.; Vanderhart, D. L. *Science* **1984**, *223*, 283–285.
(34) Earl, W. L.; VanderHart, D. L. *J. Am. Chem. Soc.* **1980**, *102*, 3251–2.
(35) Vanderhart, D. L.; Atalla, R. H. *Macromolecules* **1984**, *17*, 1465–1472.
(36) Newman, R. H. *Solid State Nucl. Magn. Reson.* **1999**, *15*, 21–29.
(37) Angelin, M.; Hermansson, M.; Dong, H.; Ramstroem, O. *Eur. J. Org. Chem.* **2006**, 4323–4326.
(38) Natansohn, A.; Yang, H.; Clark, C. *Macromolecules* **1991**, *24*, 5489–96.
(39) Pigro, M. C.; Angiuoni, G.; Piancatelli, G. *Tetrahedron* **2002**, *58*, 5459–5466.
(40) Simion, A.; Simion, C.; Kanda, T.; Nagashima, S.; Mitoma, Y.; Yamada, T.; Mimura, K.; Tashiro, M. *J. Chem. Soc., Perkin Trans. 1* **2001**, 2071–2078.
(41) Hirota, M.; Furihata, K.; Saito, T.; Kawada, T.; Isogai, A. *Angew. Chem., Int. Ed.* **2010**, *49*, 7670–7672.
(42) Saito, T.; Hirota, M.; Tamura, N.; Kimura, S.; Fukuzumi, H.; Heux, L.; Isogai, A. *Biomacromolecules* **2009**, *10*, 1992–1996.
(43) Okita, Y.; Saito, T.; Isogai, A. *Biomacromolecules* **2010**, *11*, 1696–1700.
(44) Winnik, F. M. *Polymer* **1990**, *31*, 2125–34.

BM101106C